Time scales, persistence, and dynamic mutiscaling in two-dimensional, homogeneous, isotropic fluid turbulence

Rahul Pandit

Department of Physics
Indian Institute of Science
Bangalore, India.
Kavli Institute of Theoretical Physics
31 March 2011

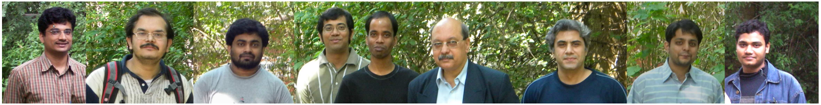

- This work has been done with
  - Dhrubaditya Mitra
  - Prasad Perlekar
  - Samriddhi Sankar Ray

- Support: CSIR, DST, UGC (India) and SERC (IISc)

References

- *Dynamic Multiscaling in Fluid Turbulence : An Overview,* D. Mitra and R. Pandit, *Physica A* **318**, 179 (2003).
- *Varieties of Dynamic Multiscaling in Fluid Turbulence,* D. Mitra and R. Pandit. *Phys. Rev. Lett.* **93**, 024501 (2004).
- *Dynamics of Passive-Scalar Turbulence,* D. Mitra, R. Pandit, *Phys. Rev. Lett.* **95**, 144501 (2005).
- *Dynamic Multiscaling in Turbulence*, R. Pandit, S. S. Ray, and D. Mitra, *Eur. Phys. J. B* **64**, 463 (2008).
- *The Universality of Dynamic Multiscaling in Homogeneous, Isotropic Navier-Stokes and Passive-Scalar Turbulence*, S. S. Ray, D. Mitra, and R. Pandit, *New J. of Phys.* **10**, 033003 (2008).
- *The Persistence Problem in Two-Dimensional Fluid Turbulence*, P. Perlekar, S. S. Ray, D. Mitra, and R. Pandit, *Phys. Rev. Lett.* **106**, 054501 (2011).
- *Dynamic Multiscaling in Two-dimensional Turbulence*, S. S. Ray, P. Perlekar, D. Mitra, and R. Pandit, *to be submitted*.

Outline

A. The persistence problem in two-dimensional fluid turbulence :

1. Motivation: The persistence problem in nonequilibrium statistical mechanics.
2. Two-dimensional fluid turbulence.
3. Okubo-Weiss parameter: A natural candidate for the study of persistence in two-dimensional fluid turbulence.
4. Calculations and results.
5. Conclusions

Outline

B. The dynamic multiscaling of time-dependent structure functions in turbulence :

1. Motivation: Critical phenomena in statistical mechanics.
2. The Universality of Dynamic Multiscaling in Homogeneous, Isotropic in Three-dimensional Turbulence.
3. Dynamic Multiscaling in Two-dimensional Fluid Turbulence.
4. Conclusions.

Two dimensional flows in nature

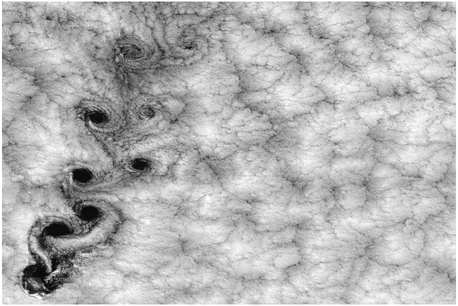

Von Kármán vortex street off the Chilean coast near the Juan Fernandez Islands.

Two dimensional flows in Jupiter atmosphere

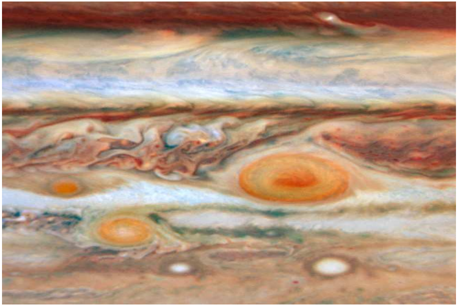

- Great red spot around 350 years old,
- Size: $2-3$ earth diameters,
- Estimated wind speeds approximately $619\mathrm{km/h}$; easily fits into Type-V hurricanes (speeds above $249\mathrm{km/h}$).

Two dimensional flow in laboratory

Soap film flow behind two cylinders

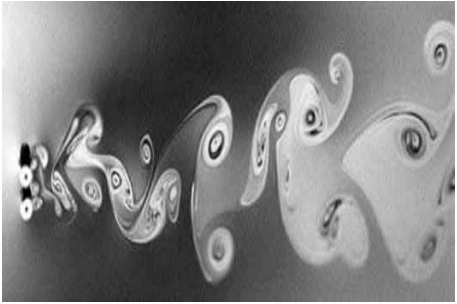

Two dimensional Navier-Stokes

Vorticity-streamfunction formulation:

- $\omega \equiv (\partial_x u_y - \partial_y u_x)$.
- $u_x \equiv -\partial_y \psi$; $u_y \equiv \partial_x \psi$.

$$\begin{aligned} D_t \omega &= \nu \nabla^2 \omega + \mathbf{f}^{\omega}, \\ \nabla^2 \psi &= \omega, \end{aligned} \tag{1}$$

- No vortex stretching; $\omega . \nabla \mathbf{u}$ is absent.

Two-dimensional Navier-Stokes: Conservation laws

[U. Frisch, Turbulence]

- Energy and enstrophy conserved in the inviscid, unforced limit.
- Energy and enstrophy balance in the unforced, viscous $2D$ NS equations

$$\begin{aligned} \partial_t E &= -2\nu\Omega, \\ \partial_t \Omega &= -2\nu P. \end{aligned}$$

where,
$E = 1/2 \int_{\mathbf{x} \in R^3} |\mathbf{u}|^2, \Omega = 1/2 \int_{\mathbf{x} \in R^3} |\omega|^2$, and
$P = 1/2 \int_{\mathbf{x} \in R^3} |\nabla \times \omega|^2$.

- $\lim \nu \to 0$, $\Omega \to const.$ and $E \to 0$. No dissipative anamoly for energy!

Two-dimensional Turbulence: Cascades

[Kraichnan, Phys. Fluids, **10**, (1967*a*), Batchelor, Phys. Fluids Suppl. *II*, **12**, (1969)]

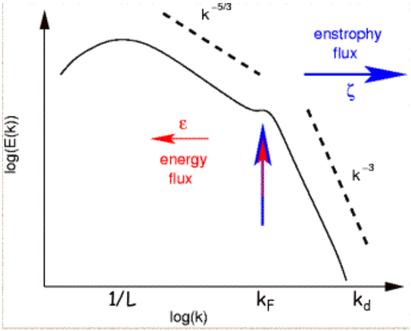

- Energy injected at a length scale l_{inj} will inverse-cascade to large length scales with $E(k) \sim k^{-5/3}$.
- Energy injected at a length scale l_{inj} will forward-cascade to small length scales with $E(k) \sim k^{-3}$.

Direct Numerical Simulation(DNS)

- Vorticity-streamfunction formulation

$$
\begin{aligned}
D_t\omega &= \nabla^2\omega - \gamma\omega + \mathcal{G}f, \\
\nabla^2\psi &= \omega, \\
\mathbf{u} &= (-\partial_y\psi, \partial_x\psi).
\end{aligned}
$$

- $\mathbf{x}' \to \mathbf{x}/\ell_{inj}$, $t' \to t\nu/\ell_{inj}^2$, $f'_\omega \to f_\omega(\ell_{inj}/||f_\omega||_2)$
- $\mathcal{G} \equiv 2\pi||f_\omega||_2/(k_{inj}^3\rho\nu^2)$ and $\gamma = \alpha/(k_{inj}^2\nu)$
- Incompressibility satisfied by construction

Persistence problem

Satya N. Majumdar, Persistence in Nonequilibrium Systems, Curent Science, **77**, 370 (1999); cond-mat/9907407v1

Let $\phi(x,t)$ be a nonequilibrium field fluctuating in space and time according to some dynamics. Persistence is simply the probability $P_0(t)$ that at a fixed point in space, the quantity $sgn[\phi(x,t) - \langle\phi(x,t)\rangle]$ does not change upto time t.

The Okubo-Weiss parameter

- From the velocity-gradient tensor $\mathcal{A}$, with components $A_{ij} \equiv \partial_i u_j$, we obtain the Okubo-Weiss parameter Λ, the discriminant of the characteristic equation for $\mathcal{A}$.
- If Λ is positive (negative) then the flow is vortical (extensional).
- In an incompressible flow in two dimensions $\Lambda = \det \mathcal{A}$; and the PDF of Λ has been shown to be asymmetrical about $\Lambda = 0$ (vortical regions are more likely to occur than strain-dominated ones).

Motivation

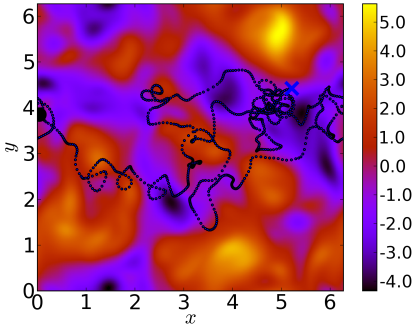

- Note $\langle \Lambda \rangle = 0$.
- How long does a Lagrangian particle stay in region where $\Lambda > 0$ (center) or where $\Lambda < 0$ (saddle).
- How long does the Λ field not change sign at a position (x, y) i.e., persistence time of a center or a saddle.

Persistence in two-dimensional turbulence

- Lagrangian persistence: We follow N_p particles and evaluate Λ along their trajectories.
- Eulerian persistence: We monitor the time evolution of Λ at N positions in the simulation domain.
- For both the cases find the time-intervals τ over which $\Lambda > 0$ or $\Lambda < 0$. The PDF of these intervals characterizes the analog of persistence in two dimensional turbulence.

Persistence-time PDF

- We denote the persistence-time PDFs by P; the subscripts E and L on these PDFs signify Eulerian and Lagrangian frames, respectively; and the superscripts $+$ or $-$ distinguish PDFs from vortical points from those from extensional ones.
- To find out the persistence-time PDF $P_E^+(\tau)$ [resp., $P_E^-(\tau)$] we analyse the time-series of Λ obtained from each of the N_p Eulerian points and construct the PDF of the time-intervals τ over which Λ remains positive (resp., negative).
- The same method applied to the time series of Λ, obtained from each of the N_p Lagrangian particles, yields $P_L^+(\tau)$ [resp., $P_L^-(\tau)$].

Simulation details

N	ν	μ	F_0	k_{inj}	l_d	λ	Re_λ	T_{E}^-	T_{L}^-	T_{E}^+
512	0.016	0.1	45	10	0.023	0.17	59.2	0.6	0.12	0.34
512	0.016	0.45	45	10	0.021	0.11	26.8	0.4	0.15	0.28
1024	10^{-5}	0.01	0.005	10	0.0043	0.125	827.3	20.0	9.9	14.28
1024	10^{-5}	0.01	0.005	4	0.0054	0.198	1318.8	33.3	12.5	25.0

Time series of Λ

Lagrangian versus Eulerian frame

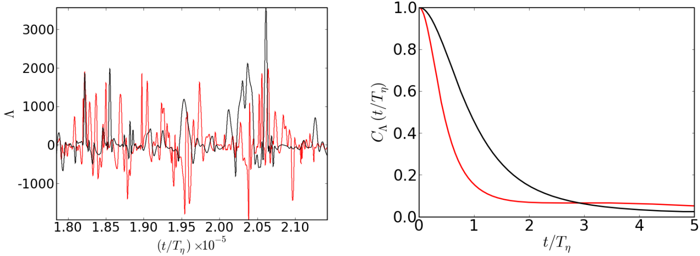

- Lagrangian Λ tracks (red) show rapid fluctuations in comparison to the corresponding Eulerian tracks (black).
- Autocorrelation $C_\Lambda = \langle \Lambda(t_0)\Lambda(t_0 + t)\rangle$ decays faster for the Lagrangian case.

Persistence: particle in a vortex

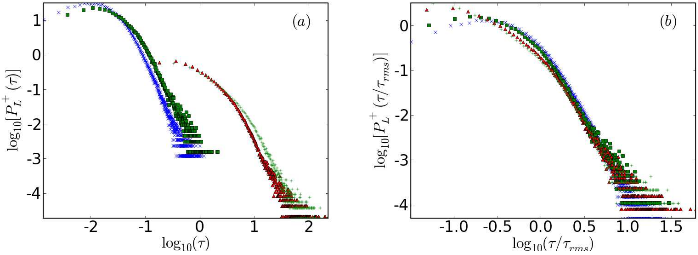

- $Re = 59.2,\ k_{inj} = 10,\ \alpha = 0.1$ (×),
- $Re = 26.8,\ k_{inj} = 10,\ \alpha = 0.45$ (□),
- $Re = 827.3,\ k_{inj} = 4,\ \alpha = 0.01$ (△),
- $Re = 1318.8,\ k_{inj} = 10,\ \alpha = 0.01$ (+).

Persistence: particle in a vortex

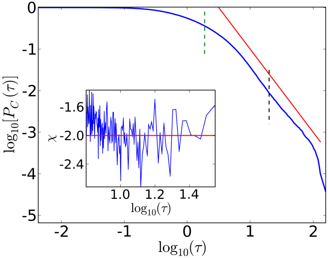

- $P^C(\tau) = \tau^{-(\beta-1)}$, $\beta = 2.9 \pm 0.2$.
- Independent of Re, k_{inj}, and α

Persistence: particle in a region of strain

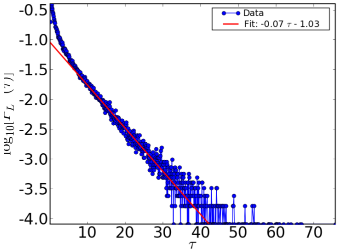

- Lin-log plot of the persistence time of the particle in a region of strain.

Persistence: Region of vorticity at (x, y)

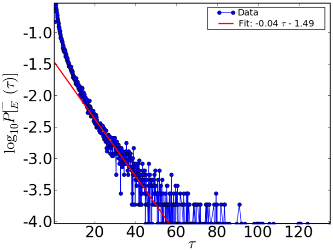

- Lin-log plot of the persistence time of the region of vorticity at position (x, y).

Persistence: Region of strain at (x, y)

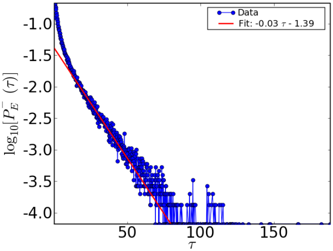

- Lin-log plot of the persistence time of the region of strain at position (x, y).

Conclusion

- The Okubo-Weiss parameter provides us with a natural way of formulating and studying the persistence problem in two-dimensional fluid turbulence.
- The persistence-time PDF of Lagrangian particles in vortical and strain-dominated regions are different.
- The persistence-time PDF of Lagrangian particles in vortical regions show a power-law tail with an exponent $\beta = 2.9$.
- The persistence-time PDF of Lagrangian particles in strain-dominated regions shows an exponential tail.

Critical Phenomena

$\Gamma(r, t, h) \approx \frac{1}{r^{d-2+\eta}} \mathcal{F}(t^{\nu}\xi, h/t^{\Delta})$

- r: separation between the spins in d dimensions
- $t \equiv (T - T_c)/T_c$
- $h \equiv H/k_B T_c$
- k_B: Boltzmann constant
- T: temperature
- T_c: critical temperature
- H: magnetic field
- ξ: correlation length (diverges at criticality)
- η, ν and Δ: static critical exponents
- $\mathcal{F}$: universal scaling function

Critical Phenomena

In Fourier space
$\tilde{\Gamma}(q, t, h) \approx \frac{1}{q^{2-\eta}} \mathcal{F}(t^{\nu}\xi, h/t^{\Delta})$;
$\vec{q}$: wave vector with magnitude q
Dynamic scaling for time-dependent correlation functions in the vicinity of a critical point.
$\tilde{\Gamma}(q, \omega, t, h) \approx \frac{1}{q^{2-\eta}} \mathcal{G}(q^{-z}\omega, t^{\nu}\xi, h/t^{\Delta})$;

- z: dynamic critical exponent
- ω: frequency
- $\mathcal{G}$: a scaling function

Relaxation time τ diverges as

$$\tau \sim \xi^{z}.$$

Equal-Time Structure Functions

- Order-p, equal-time, structure functions:

$$\mathcal{S}_p(r) \equiv \langle [\delta u_\parallel(\vec{x}, \vec{r}, t)]^p \rangle \sim r^{\zeta_p}$$

$$\delta u_\parallel(\vec{x}, \vec{r}, t) \equiv [\vec{u}(\vec{x} + \vec{r}, t) - \vec{u}(\vec{x}, t)] \cdot \frac{\vec{r}}{r}$$

  η_d: Kolmogorov dissipation scale;
  L: large length scale at which energy is injected into the system.

- Experiments favour multiscaling: ζ_p a nonlinear, convex monotone increasing function of p.
- Simple-scaling prediction of Kolmogorov: $\zeta_p^{K41} = p/3$.

Introduction : Frames of Reference

- **Eulerian** :
  The Navier-Stokes equation is written in terms of the Eulerian velocity $\mathbf{u}$ at position $\mathbf{x}$ and time t. In the Eulerian case the frame of reference is fixed with respect to the fluid;
- **Lagrangian** :
  Frame of reference fixed to a fluid *particle*; this fictitious particle moves with the flow and its path is known as a Lagrangian trajectory.

$$\mathbf{v} = \left(\frac{d\mathbf{R}}{dt} \right)_{\mathbf{r_0}};$$

- **Quasi-Lagrangian** :
  It uses the following transformation for an Eulerian field $\psi(\mathbf{r}, t)$:

$$\hat{\psi}(\mathbf{r}, t) \equiv \psi[\mathbf{r} + \mathbf{R}(t; \mathbf{r_0}, 0), t].$$

Time-Dependent Structure Functions

- The order-p, time-dependent longitudinal structure function:

  $$\mathcal{F}_p(r, \{t_1, \ldots, t_p\}) \equiv \langle [\delta u_\parallel(\vec{x}, t_1, r) \ldots \delta u_\parallel(\vec{x}, t_p, r)] \rangle$$

  For simplicity we consider $t_1 = t$ and $t_2 = \ldots = t_p = 0$.

- Given $\mathcal{F}(r, t)$, different ways of extracting time scales yield different exponents that are defined via dynamic-multiscaling ansätze:

$$\mathcal{T}_p(r) \sim r^{z_p}.$$

The GOY Shell Model

The evolution equation for the GOY shell model takes the form,

$$[\frac{d}{dt} + \nu k_n^2]u_n = i(a_n u_{n+1} u_{n+2} + b_n u_{n-1} u_{n+1} + c_n u_{n-1} u_{n-2})^* + f_n.$$

- In the shell model equation,
  - $k_n = k_0 2^n$, where $k_0 = 1/16$;
  - $a_n = k_n$, $b_n = -\delta k_{n-1}$, $c_n = -(1-\delta)k_{n-2}$, where $\delta = 1/2$.

Simulation Details

- We use the slaved Adams-Bashforth scheme to integrate the GOY shell model equation with 22 shells.
- We use $\delta t = 10^{-4}$ and $\nu = 10^{-7}$.
- For statistically steady turbulence, we use external forcing to drive the system.
- We study decaying turbulence by using two kinds of initial conditions:
  1. a random configuration where all the energy is concentrated at large length scales;
  2. a configuration obtained from a statistically steady turbulent state.

Details: Forced Turbulence

- We start from an initial condition where all the energy is concentrated in the large length scales, i.e., $v_n^0 = k_n^{-1/3} e^{i\theta_n}$ (for n = 1,2) and $v_n^0 = 0$ (for n = 3 to 22), with θ_n a random phase angle distributed uniformly between 0 and 2π.
- The system is then driven to a statistically steady state with a force $f_n = \delta_{n,1}(i + i) \times 5 \times 10^{-3}$.
- All measurements are made once the system reaches a statistically steady state.

Details: Decaying Turbulence

- For the first initial condition we use $v_n^0 = k_n^{1/2} e^{i\theta_n}$ (for n $=$ 1,2) and $v_n^0 = k_n^{1/2} e^{-{k_n}^2} e^{i\theta_n}$ (for n $=$ 3 to 22) with θ_n a random phase angle distributed uniformly between 0 and 2π.
- For the second initial condition, we first achieve a forced statistically steady state, with $f_n = \delta_{n,1}(i+i) \times 5 \times 10^{-3}$. The force is then switched off at some time origin t_0 and the system is allowed to decay freely.
- Our exponents are independent of the kind of initial condition we choose.

Error Estimates (GOY)

- Static solution exhibit a 3-cycle in the shell index n.
- Obtain 50 different values of each of the exponents from 50 independent simulations.
- Time-averaging is done over a time $T_{av} = 10^5 \times \tau_L$ to obtain the results for statistically steady state quantities. For decaying turbulence, we average over 20000 statistically independent initial configurations.
- The means of these 50 values for each of the dynamic-multiscaling exponents are shown in figure and the standard deviation yields error.
- This averaging is another way of removing the effects of the 3-cycle mentioned above.

Principal Results: Fluid Turbulence

- Simple dynamic scaling for Eulerian-velocity structure functions ($z_p^E = 1$).
- Dynamic multiscaling is obtained for Lagrangian or Quasi-Lagrangian structure functions.
- Dynamic multiscaling exponents z_p depend on how $\mathcal{T}_p(r)$ is extracted.
- z_p is related to the equal-time exponents via bridge relations.
- Universality of dynamic exponents: the same for decaying and statistically steady turbulence.

Integral Time Scale

- From the longitudinal, time-dependent, order-p structure functions, the order-p, degree-M, integral time scale is defined as,

$$\mathcal{T}^{I}_{p,M}(r) \equiv \left[\frac{1}{\mathcal{S}_p(r)} \int_0^{\infty} \mathcal{F}_p(r,t) t^{(M-1)} dt\right]^{(1/M)}$$

- The integral dynamic multiscaling exponent $z^{I}_{p,M}$ is defined as

$$\mathcal{T}^{I}_{p,M}(r) \sim r^{z^{I}_{p,M}}.$$

Derivative Time Scale

- Similarly, the order-p, degree-M derivative time scale is defined as

$$\mathcal{T}^D_{p,M}(r) \equiv \left[\frac{1}{\mathcal{S}_p(r)} \frac{\partial^M \mathcal{F}_p(r,t)}{\partial t^M}\right]^{(-1/M)}$$

- The derivative dynamic multiscaling exponent $z^D_{p,M}$ is defined as

$$\mathcal{T}^D_{p,M}(r) \sim r^{z^D_{p,M}}.$$

Theoretical Prediction

- The multifractal model predicts the following bridge relations:

$$z^{I}_{p,M} = 1 + \frac{[\zeta_{p-M} - \zeta_p]}{M};$$

$$z^{D}_{p,M} = 1 + \frac{[\zeta_p - \zeta_{p+M}]}{M}.$$

Extending the Frisch-Parisi Multifractal Model

Dynamic Structure Functions

$$\mathcal{F}_p(\ell, t) \propto \int_{\mathcal{I}} d\mu(h) (\frac{\ell}{L})^{\mathcal{Z}(h)} \mathcal{G}^{p,h}(\frac{t}{\tau_{p,h}}),$$

where $\mathcal{G}^{p,h}(\frac{t}{\tau_{p,h}})$ has a characteristic decay time $\tau_{p,h} \sim \ell/\delta v(\ell) \sim \ell^{1-h}$, and $\mathcal{G}^{p,h}(0) = 1$. If $\int_0^\infty t^{(M-1)} \mathcal{G}^{p,h} dt$ exists, then the order-p, degree-M, integral time scale is

$$\mathcal{T}^I_{p,M}(\ell) \equiv \left[\frac{1}{\mathcal{S}_p(\ell)} \int_0^\infty \mathcal{F}_p(\ell, t) t^{(M-1)} dt \right]^{(1/M)}.$$

* V.S. L'vov, E. Podivilov, and I. Procaccia, Phys. Rev. E **55**,7030 (1997).

Multifractal Model

$$\mathcal{T}^{I}_{p,1}(\ell) \equiv \left[\frac{1}{\mathcal{S}_p(\ell)}\int_0^\infty \mathcal{F}_p(\ell,t)dt\right]^{(1/M)}$$

$$\propto \left[\frac{1}{\mathcal{S}_p(\ell)}\int_{\mathcal{I}} d\mu(h)(\frac{\ell}{L})^{\mathcal{Z}(h)}\int_0^\infty dt\mathcal{G}^{p,h}(\frac{t}{\tau_{p,h}})\right]$$

$$\propto \left[\frac{1}{\mathcal{S}_p(\ell)}\int_{\mathcal{I}} d\mu(h)(\frac{\ell}{L})^{ph+3-D(h)}\ell^{1-h}\right]$$

In the last step, we have used :

$$\tau_{p,h} \sim \ell/\delta v(\ell) \sim \ell^{1-h}$$

Multifractal Model

- Corresponding Bridge Relations :

$$z^{I}_{p,1} = 1 + [\zeta_{p-1} - \zeta_p],$$

$$z^{D}_{p,2} = 1 + [\zeta_p - \zeta_{p+2}]/2.$$

- Bridge relations reduce to $z^{K41}_p = 2/3$ if we assume K41 scaling for the equal-time structure functions.

Numerical studies of dynamic multiscaling

- L. Biferale, G. Bofetta, A. Celani, and F. Toschi, Physica D **127** 187 (1999); this study uses an exit-time method.
- Our group has concentrated on an elucidation of dynamic multiscaling by using time-dependent structure functions and
  (a) shell models and
  (b) the two-dimensional Navier-Stokes equation with Ekman friction.

In the following slides we give an overview of our results without technical details.

Results

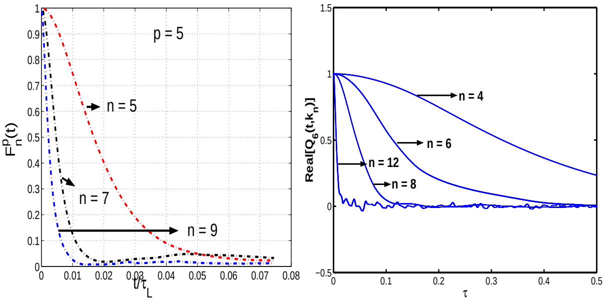

Plots of order-p structure functions *vs* the dimensionless time for various shells for statistically steady (left) and decaying (right) turbulence.

Integral Time Scales

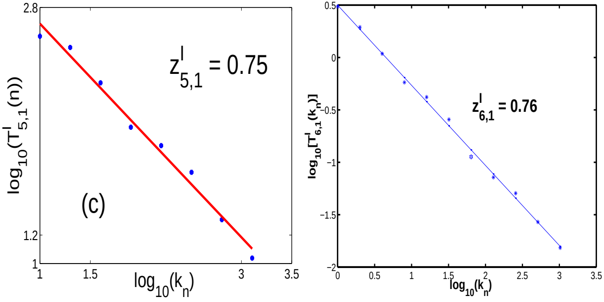

Log-log plots of integral times for statistically steady (left) and decaying (right) turbulence for order-p structure functions; the slopes of these graphs yield $z^I_{p,1}$. The integration is carried out over time 0 to t_u, where we choose t_u such that $F_p(n, t_u)$ (or $Q_p(n, t_u)) = \alpha$ for all n and p.

Derivative Time Scales

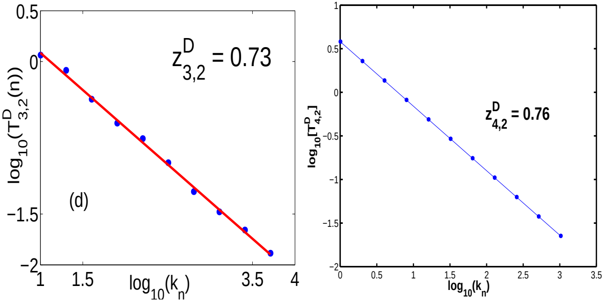

The analogue of the previous figure for derivative time scales yields $z^D_{p,1}$. We use a centered, sixth-order, finite-difference scheme by extending $F_p(n,t)$ (or $Q_p(n,t)$) to negative t via $F_p(n,-t)$(or $Q_p(n,-t)) = F_p(n,t)$(or $Q_p(n,t)$) to obtain the derivative time scales.

Passive Scalars

- We use two different kinds of velocity fields in the advection-diffusion equation for both statistically steady and decaying turbulence:
  - Model A : The Kraichnan ensemble where each component of $\mathbf{u}$ is a zero-mean, delta-correlated Gaussian random variable.
  - Model B : Velocities from the GOY shell model.

Principal Results: Passive-Scalars

- Dynamic multiscaling is obtained only if the advecting velocity is intermittent.
- Simple dynamic scaling is obtained for a simple version of the passive-scalar problem (Kraichnan), in which the advecting velocity field is Gaussian, even though equal-time structure functions display multiscaling in this model.
- For intermittent velocity fields, different time scales can be extracted.
- z_p related to ζ_p through bridge relations.
- Universality: Dynamic exponents for decaying and statistically steady passive-scalar turbulence are equal.

Model A

- The covariance of the field is

$$< u_i(\mathbf{x},t)u_j(\mathbf{x}+\mathbf{r},t') >= 2D_{ij}\delta(t-t')$$

where the Fourier Transform of D_{ij} has the form

$$\tilde{D}_{ij}(\mathbf{q}) \propto \left(q^2 + \frac{1}{L^2}\right)^{-(d+\xi)/2} e^{-\eta q^2}\left[\delta_{ij} - \frac{q_i q_j}{q^2}\right].$$

In the limits $L \longrightarrow \infty$ and $\eta \longrightarrow 0$, D_{ij} in real space is

$$D_{ij}(\mathbf{r}) = D^0\delta_{ij} - \frac{1}{2}d_{ij}(\mathbf{r}))$$

where,

$$d_{ij} = D_1 r^{\xi}\left[(d-1+\xi)\delta_{ij} - \xi\frac{r_i r_j}{r^2}\right]$$

Passive-scalar shell models

$$\left[\frac{d}{dt} + \kappa k_n^2\right]\theta_n = \imath\Big[a_n(\theta^*_{n+1}u^*_{n-1} - \theta^*_{n-1}u^*_{n+1}) + b_n(\theta^*_{n-1}u^*_{n-2} + \theta^*_{n-2}u_{n-1}) + c_n(\theta^*_{n+2}u_{n+1} + \theta^*_{n+1}u^*_{n+2})\Big] + f_n,$$

where the asterisks denote complex conjugation, $a_n = k_n/2$, $b_n = -k_{n-1}/2$, and $c_n = k_{n+1}/2$; f_n is an additive force that is used to drive the system to a steady state; the boundary conditions are $u_{-1} = u_0 = \theta_{-1} = \theta_0 = 0; u_{N+1} = u_{N+2} = \theta_{N+1} = \theta_{N+2} = 0$.

- For the Kraichnan model, the advecting velocity variables are taken to be zero-mean, white-in-time, Gaussian random complex variables with covariance $\langle u_n(t)u^*_m(t')\rangle = C_2 k_n^{-\xi}\delta_{mn}\delta(t - t')$.
- For a "turbulent" passive-scalar field, the advecting velocity field is a solution of the GOY shell model.

Model A

This model shows multiscaling for equal-time passive-scalar structure functions for $0 < \xi < 2$.

Dynamic Multiscaling in Passive-Scalars

Multifractal model predicts:

- $z^D_{p,M} = 1 - \zeta^u_M/M$
- $z^I_{p,M} = 1 - |\zeta^u_{-M}|/M$
- Breakdown of simple scaling.
- Does structure functions with negative exponents exists?

Analytical and Numerical Results

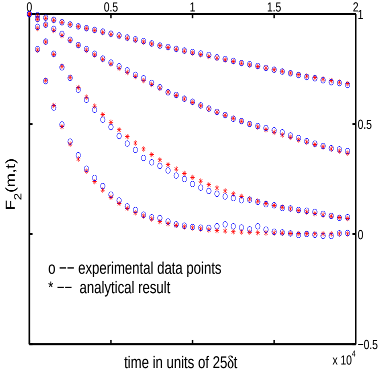

A comparison of our numerical and analytical results for model A second-order structure function in decaying turbulence.

Model A: Numerical Results

- Analytical work shows that for Model A the time-dependent structure functions decay exponentially.
- A log-log plot of the characteristic decay time *vs* the wave vectors yield the dynamic exponent z_p.
- It is shown analytically that for all order-p time-dependent structure functions, $z_p = 2 - \xi$.
- Our numerics support this prediction for decaying passive-scalar fields.

Model A: Numerical Results

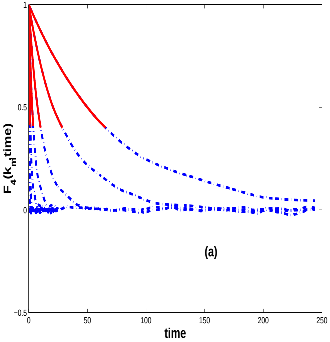

A plot of the fourth-order structure function ($\xi = 0.6$) *vs* time for statistically steady turbulence. The scaling exponent is extracted from the decay constant of the curves.

Model A: Numerical Results

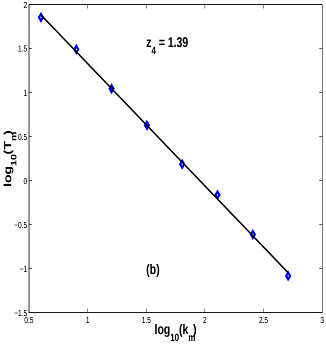

The slope of a log-log plot of the decay constant *vs* the wave-vector yields the dynamic scaling exponent for the fourth-order structure function.

Model A: Numerical Results

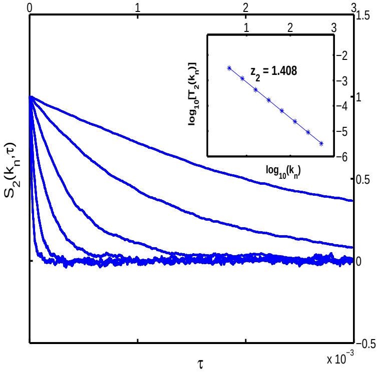

A plot of the second-order dynamic structure function for decaying turbulence. The slope of a log-log plot (inset) of the decay time *vs* the wave-vector yields the dynamic exponent .

Model B: Numerical Results

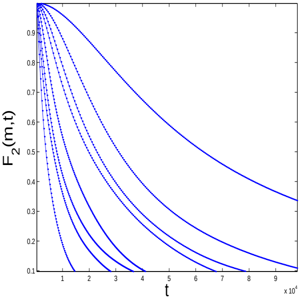

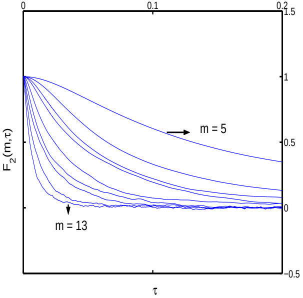

Plots of the second-order time-dependent structure function *vs* the dimensionless time for statistically steady (left) and decaying turbulence (right).

Cumulative pdf for u_m

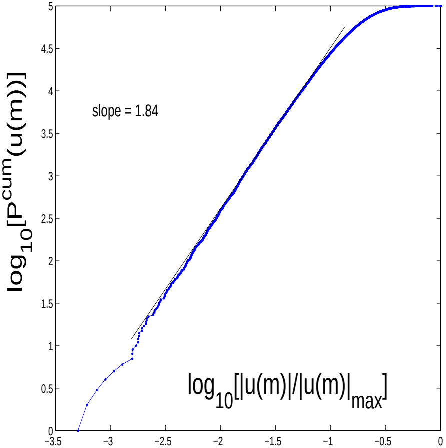

Negative Exponents

- For small $|u_m|$, $P^{cum}[|u_m|] \sim |u_m|^{1.8}$.
- $P[|u_m|] \sim |u_m|^{0.8}$.
- $S_{-1}(m) \equiv \int P[x]\frac{1}{x}dx \sim \int x^{-0.2}dx$ exists.
- But $S_p(m)$ for $p \approx -1.8$ does not.
- $T^I_{p,M}$ for $M > 2$ does not exist.
- Measurement of a static quantity $(P(x))$ gives us information about existence of a dynamic quantity $T^I_{p,M}$.

Model B: Integral Time Scale

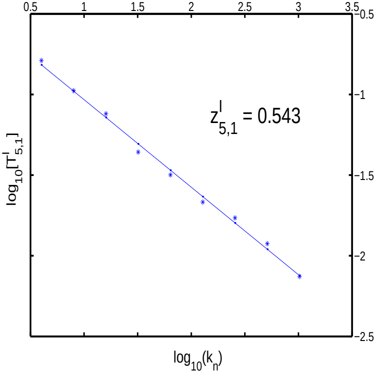

A log-log plot of the integral time scale *vs* the wave-vector in decaying turbulence. The linear fit gives us the scaling exponent $z^I_{p,M}$.

Derivative Time Scale

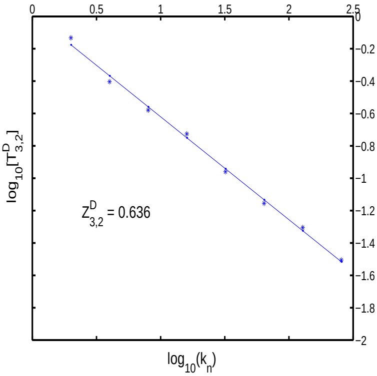

A log-log plot of the derivative time scale *vs* the wave-vector in decaying turbulence. The linear fit gives us the scaling exponent $z^D_{p,M}$.

Exponents for dynamic multiscaling in shell models

order(p)	ζ_p^u	$z_{p,1}^{I,u}$[Theory]	$z_{p,1}^{I,u}$	$z_{p,2}^{D,u}$[Theory]	$z_{p,2}^{D,u}$
1	0.379 $\pm$ 0.008	0.621 $\pm$ 0.008	0.61 $\pm$ 0.03	0.68 $\pm$ 0.01	0.699 $\pm$ 0.008
2	0.711 $\pm$ 0.002	0.66 $\pm$ 0.01	0.68 $\pm$ 0.01	0.716 $\pm$ 0.008	0.723 $\pm$ 0.006
3	1.007 $\pm$ 0.003	0.704 $\pm$ 0.005	0.711 $\pm$ 0.001	0.74 $\pm$ 0.01	0.752 $\pm$ 0.005
4	1.279 $\pm$ 0.006	0.728 $\pm$ 0.009	0.734 $\pm$ 0.002	0.76 $\pm$ 0.02	0.76 $\pm$ 0.01
5	1.525 $\pm$ 0.009	0.75 $\pm$ 0.02	0.755 $\pm$ 0.002	0.77 $\pm$ 0.02	0.77 $\pm$ 0.02
6	1.74 $\pm$ 0.01	0.78 $\pm$ 0.02	0.78 $\pm$ 0.03	0.77 $\pm$ 0.03	0.78 $\pm$ 0.02

order(p)	ζ_p^θ	$z_{p,1}^{I,\theta}$	$z_{p,2}^{D,\theta}$
1	0.342 $\pm$ 0.002	0.522 $\pm$ 0.002	0.632 $\pm$ 0.003
2	0.634 $\pm$ 0.003	0.531 $\pm$ 0.004	0.647 $\pm$ 0.003
3	0.873 $\pm$ 0.003	0.553 $\pm$ 0.006	0.646 $\pm$ 0.003
4	1.072 $\pm$ 0.004	0.563 $\pm$ 0.003	0.642 $\pm$ 0.005
5	1.245 $\pm$ 0.004	0.562 $\pm$ 0.006	0.643 $\pm$ 0.006
6	1.370 $\pm$ 0.006	0.576 $\pm$ 0.006	0.640 $\pm$ 0.005

Dynamic Multiscaling in Two-dimensional Fluid Turbulence

Multiscaling and quasi-Lagrangian Structure Functions

- Multiscaling in equal-time, Eulerian vorticity structure functions.
- Dynamic-multiscaling in time-dependent vorticity structure functions for Eulerian and quasi-Lagrangian fields.
- Tracking a single particle in a $2D$ flow with Ekman friction to generate quasi-Lagrangian fields.

Movie

Steady State quasi-Lagrangian Vorticity Field

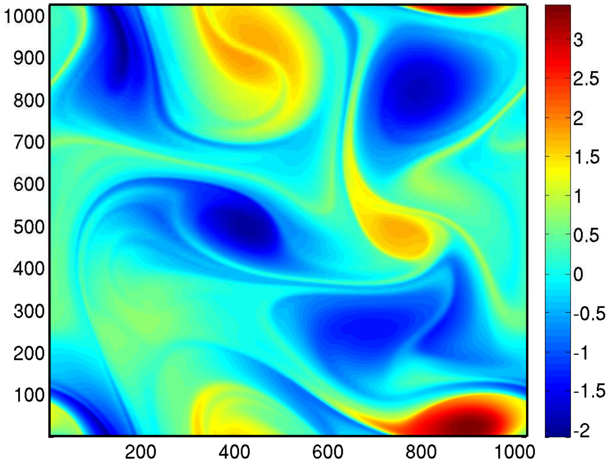

A pseudocolor plot of the quasi-Lagrangian vorticity field in the statistically steady state.

Equal-time Structure Functions

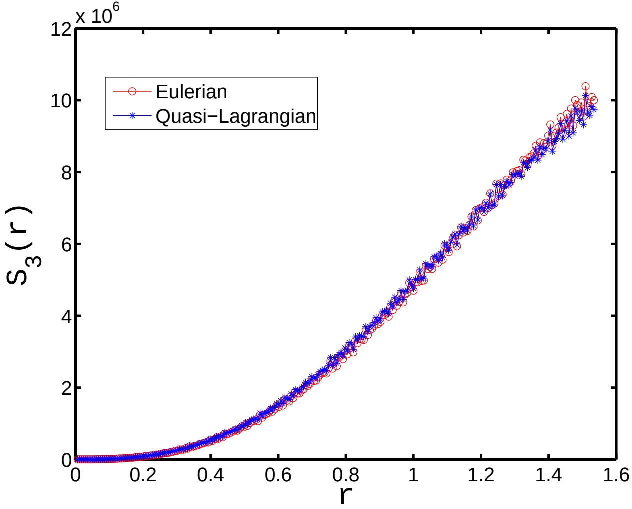

The third order structure function for the Eulerian (red) and quasi-Lagrangian (blue) fields.

Equal-time Structure Functions : quasi-Lagrangian

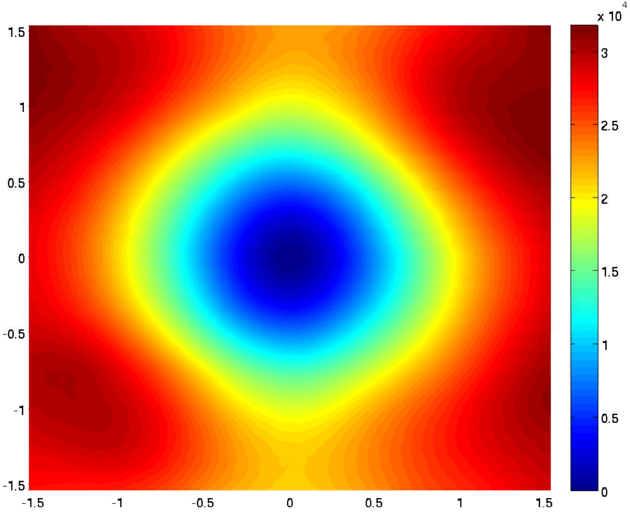

The isotropic sector for the third order structure function for the quasi-Lagrangian field.

Equal-time Exponents for Vorticity Structure Functions

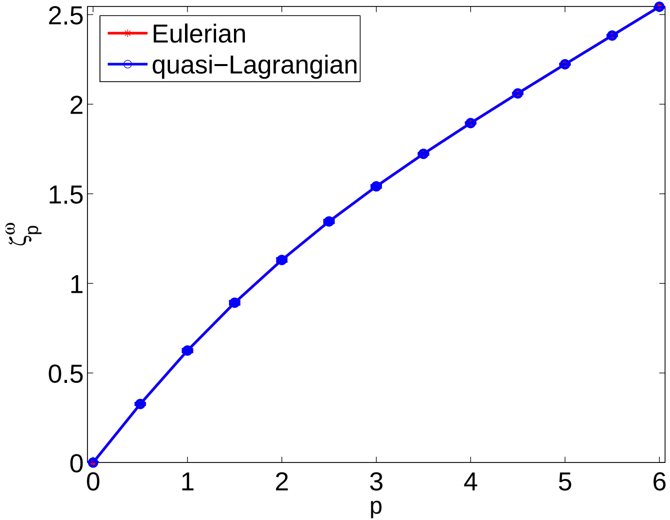

The equal-time exponents ζ_p, for the vorticity field, versus p for Eulerian (in red) and quasi-Lagrangian (in blue) fields.

Time-dependent Structure Functions

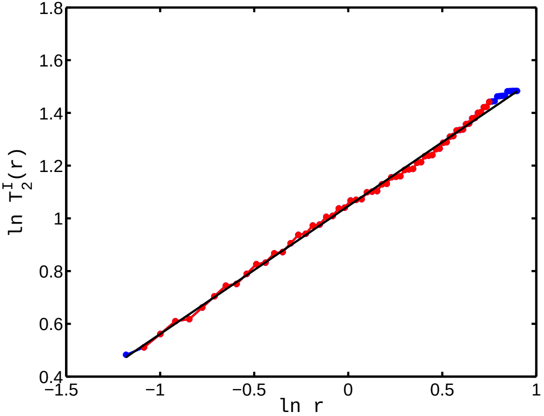

A log-log plot of $T^I_{2,1}$ versus the separation r; the data points are shown by open red circles and the straight black line shows the line of best fit in the inertial range.

Exponents from 2D DNS

order(p)	ζ_p^{qL}	$z_{p,1}^{I,\mathrm{qL}}$[Theory]	$z_{p,1}^{I,\mathrm{qL}}$	$z_{p,2}^{D,\mathrm{qL}}$[Theory]	$z_{p,2}^{D,\mathrm{qL}}$
1	0.625 ± 0.003	0.375 ± 0.007	0.37 ± 0.02	0.541 ± 0.008	0.53 ± 0.02
2	1.131 ± 0.005	0.49 ± 0.02	0.48 ± 0.01	0.618 ± 0.009	0.62 ± 0.2
3	1.541 ± 0.005	0.58 ± 0.01	0.57 ± 0.01	0.66 ± 0.01	0.67 ± 0.01
4	1.895 ± 0.004	0.65 ± 0.01	0.65 ± 0.01	0.675 ± 0.008	0.66 ± 0.03
5	2.222 ± 0.008	0.67 ± 0.01	0.65 ± 0.02	0.70 ± 0.01	0.70 ± 0.02
6	2.544 ± 0.004	0.68 ± 0.01	0.66 ± 0.02	0.71 ± 0.02	0.71 ± 0.03

Effect of Ekman Friction

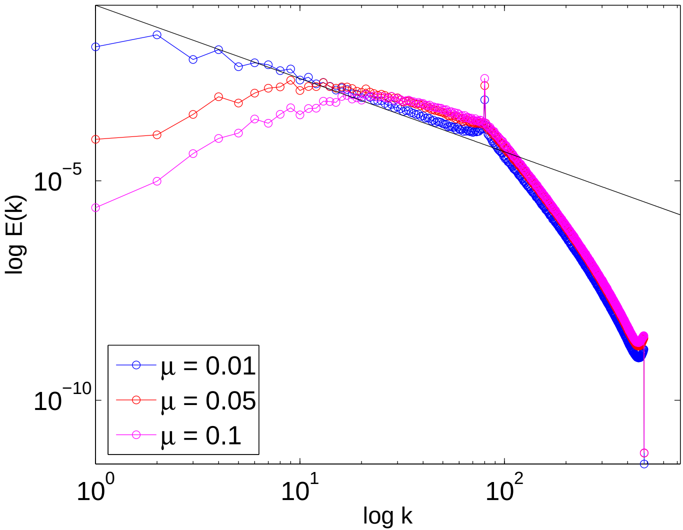

A log-log plot of the energy spectrum versus the wavevector k for various values of μ.

Conclusions

- We have checked that bridge relations hold for the vorticity structure functions in the forward cascade in 2D turbulence.
- We have also studied time-dependent structure functions in a shell model for MHD turbulence (with S.S. Ray and G. Sahoo); but here it is not clear how to obtain bridge relations.